Manganese effect on room and cryogenic temperature impact toughness of thermomechanical processed Fe-Mn binary alloys and commercial 9wt% Nickel alloy

Lebedike Mampuru[1, 2], *Desmond* Klenam[2], *Michael* Bodunrin[2], *Joseph* Moema[1], and *Maje* Phasha[1]

[1]Advanced Materials Division, MINTEK, Private bag X 3015, Randburg, 2125, South Africa
[2]University of Witwatersrand, Faculty of Engineering, School of Chemical and Metallurgical Engineering, Johannesburg, Gauteng, South Africa

Abstract. High FeMn-based alloys are explored worldwide for lightweighting in the energy, automotive and marine industries. Their desirable properties like lower density, high toughness and tensile strength, make them preferred candidates to consider for such applications. In the energy sector, this type of structural material has the potential to be used in the construction of storage and transportation tanks for liquified natural gas (LNG). LNG has been identified as one of the alternative energy sources to ease pressure on the already strained supply. The high cost and complexity of producing current alloys used in LNG storage, such as 9 wt.% Ni alloy prompted the need to explore high FeMn-based alloys. In this study, binary FeMn-based alloys produced via casting are explored. They were hot rolled and heat treated to compare their properties to those of 9 wt.% Nickel alloy. Preliminary properties measured at both room and cryogenic temperatures revealed that impact toughness increased with increasing Mn content.

1 Introduction

High manganese (Mn) based Fe-Mn alloys are explored worldwide for lightweighting in the energy, automotive and marine industries. Their desirable properties like lower density relative to the currently used materials, high toughness and tensile strength, make them preferred candidates to consider for such applications. The attractive characteristics of high Mn based Fe-Mn alloys are based on two competing deformation mechanisms emanating from the face-centred cubic (FCC) austenite phase, namely, twinning-induced plasticity (TWIP) and transformation-induced plasticity (TRIP) effects [1]. TWIP mechanism is observed during plastic deformation of Mn steels containing more than 20 weight percent (wt.%) Mn due to the high stacking faults energy (SFE) [1, 2], leading to a combination of desirable mechanical properties such as high elongation (ductility), and moderate strength higher than that of austenitic stainless steels. On the other hand, TRIP is mostly observed in Fe-Mn steels with Mn content lower than 20 wt.%, attributed to martensitic transformation from FCC (γ) to ε-hexagonal close-packed (HCP) crystal structure enabled by low SFE.

In the energy sector, the interest in exploring these materials stems from their potential use as structural materials for the construction of storage and transportation tanks and pipes for liquified natural gas (LNG).

LNG has been identified as one of the alternative energy sources to ease pressure on the already strained energy supply [3, 4]. The introduction of LNG as an alternative energy source comes with new infrastructure requirements. The construction of large tanks and long pipelines for the storage and transportation of LNG requires a large quantity of specialised commercial steels such as 9 wt. % nickel (Ni) and 304 stainless steels. Despite their high cost because of Ni content, these specialised steels are used because of the high strength and toughness required in these applications, especially at sub-zero (-196 °C) temperatures. These materials are found to be suitable for use in these cryogenic conditions, however, the metallurgical processes employed to produce them are complex, leading to high costs due to limited availability [1, 2, 4]. Hence, the exploration of high Mn based FeMn alloys as potential alternative alloys that could be cheaper and relatively easier to produce.

In this paper, the mechanical properties of hot-rolled and heat-treated binary Fe-Mn alloys with Mn content varying from 22, 25, 30 and 35 wt.% are explored as an entry point to this application and are compared to the 9 wt.% Ni alloy as a reference material. The focus is mainly on the assessment of the room and cryogenic temperature toughness of the binary Fe-Mn alloys.

2 Methodology

2.1 Alloy casting and processing

Melting and casting were done using a 50 kg medium-frequency induction furnace. The induction furnace was fitted with an alumina cast crucible, which was backfilled with MR21 (Magnesia-chrome) ramming refractory material. The crucible was installed and baked for a few hours before the casting to remove any moisture, which would be deleterious to the casting process. The binary alloys were cast in the form of 20 kg ingots. The ingots were cast into an open silica gel-bonded sand mould. Their dimensions were (length by thickness) 260 mm x 45 mm as per Figure 1(a). This was done in the open air. Lollipop samples were also cast for chemical composition analysis. The chemical compositions of the alloys were confirmed by the spark emission spectrometry using the SpectroMAXx metal analyser machine, and the compositions of the alloys are in Table 1.

Table 1. Chemical composition of the cast binary Fe-Mn alloy compositions and 9% Ni alloy.

Alloy Name	**Chemical Composition wt%**								
	C	**Si**	**Mn**	**S**	**P**	**Ni**	**Al**	**Cr**	**Fe**
In-house Reference (Ref)	0.13 max	0.13 - 0.45	0.98	0.015	0.015	8.5-9.6	0.01	0.01	Remainder
A1	0.03	0.23	22	0.006	0.009	0.04	0.002	0.21	
A2	0.02	0.23	25	0.007	0.007	0.03	0.001	0.22	
A3	0.03	0.22	30	0.005	0.007	0.03	0.003	0.18	
A4	0.03	0.26	35	0.006	0.009	0.04	0.002	0.29	

The thermomechanical processing (hot rolling) was conducted by rolling from 45 mm-thick ingots to 12.5 mm plates as per the parameters in Table 2. The ingots were heated to 1200 °C in a muffle furnace and held for 2 hours, then rolled from 45 mm through to 21 mm and returned to the furnace for 20 minutes. After 20 minutes of soaking, they were rolled down to 12.5 mm gauge for three passes, then water quenched. This rolling schedule is also presented

as a schematic in Figure 1 (b), and the rolled ingots as plates after rolling are shown in Figure 1 (c).

Table 2. The parameters for the thermomechanical processing of the ingots.

No. Passes	Temp.(°C)	Sample Thickness (Before pass) (mm)	Sample Thickness (After Pass) (mm)	Reduction (mm)	Strain (%)
1x Pass	1200	45	35	10.0	23
1x Pass	990	35	27	8.0	
1x Pass	867	27	21	6.0	
3x Pass	1200	21	12.5	8.5	40

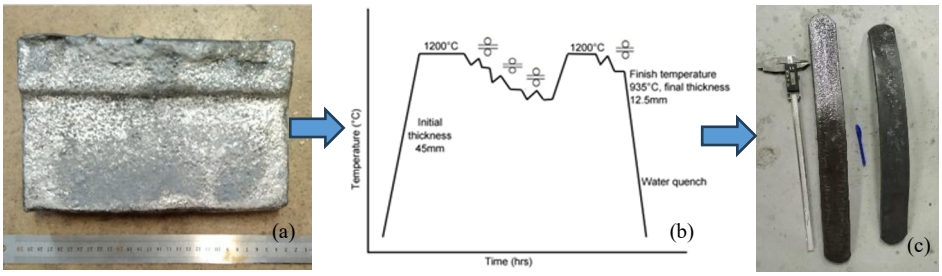

Fig. 1. (a) A representative ingot in the as-cast condition, (b) thermomechanical processing schedule and (c) ingots as plates after the rolling schedule.

The ingots, which are now plates, were double normalised and tempered according to the schedule in Table 3. This is the schedule used for the composition of the Reference Alloy. These plates were first normalised at 900 °C for 1 hour and cooled in air, then reheated to 790 °C for 1 hour and cooled in air, followed by tempering at 565 °C for 1 hour and air cooled.

Table 3. The heat treatment schedule of the rolled plates.

HT Step	Temperature (°C)	Duration
First Normalising	900	1 hour
Second Normalising	790	1 hour
Tempering	565	1 hour

2.2 Microstructure, hardness and impact testing

Specimens were sectioned from the alloys in preparation for microstructural analysis. They were hot mounted, ground and polished and etched with 2% Nital for microstructural study. Charpy specimens were extracted from the alloys using a wire cutting technique, with the cut made along the longitudinal direction. Charpy Impact toughness testing was done using the Instron MPX motorised pendulum impact tester. This test was conducted at room and subzero temperatures (-196 °C). Vickers hardness was done on the specimen using an EMCOTest Duravision hardness testing machine using a load of 10 kgf.

This paper will mainly focus on the microstructure and impact of the heat-treated (HT) alloys, as well as the hardness and impact of the hot rolled HR. The impact at cryogenic temperature for HR and HT is also highlighted. The HR microstructures were discussed in the previous work [5].

3 Results and discussion

3.1 Microstructures

The microstructures of the specimens from the hot-rolled and heat-treated plates were analysed and compared to the expected literature results. The microstructure of the Reference alloy was first presented in the as-cast, rolled and heat-treated state for demonstration of the heat treatment effect. Although the heat treatment is designed for the Reference alloy, it was also used on the binary alloys to assess its effectiveness before designing an aligned one for the Fe-Mn alloy.

One can observe the distinct difference in the morphology of the microstructure of the Reference material in the as-cast, rolled and heat-treated conditions. The as-cast microstructure consists of the darkened primary phase of martensite and interdendritic regions containing the secondary light phase of austenite, Fig.2 (left). The rolled sample of the Reference showed banding lines that follow the rolling direction; the matrix of the rolled Reference consists of martensite and retained austenite, Fig. 2 (middle). Fig. 2 (right) is the heat-treated Reference's microstructure consisting of martensitic (brown) matrix with patches of retained austenite (lighter areas), which is crucial for this composition since it helps provide the toughness needed for use at extremely low temperatures [5]. The microstructure of the heat-treated Reference is comparable to the literature.

An austenitic (γ) matrix was observed in the hot rolled binary alloys (A1 through A4), and within the grains, tangled lines were present, which may be twin bands, slip bands, or (ε) martensite bands, Fig. 3. Rolling marks were clearly observed horizontally across the alloys, which are parallel to the rolling direction. According to literature, high manganese type of alloys with a compositional content of above 16 wt.% Mn are either a mixture of γ and ε or a single-phase austenite [5].

The stability of the austenite phase in the Fe-Mn binary system is greatly enhanced by increasing the manganese (Mn) concentration. Face-centred cubic (FCC) austenitic structures are thermodynamically stable over a wider temperature range when manganese is present because it is a potent austenite-stabilising element [6]. Further microstructural synthesis is required using SEM.

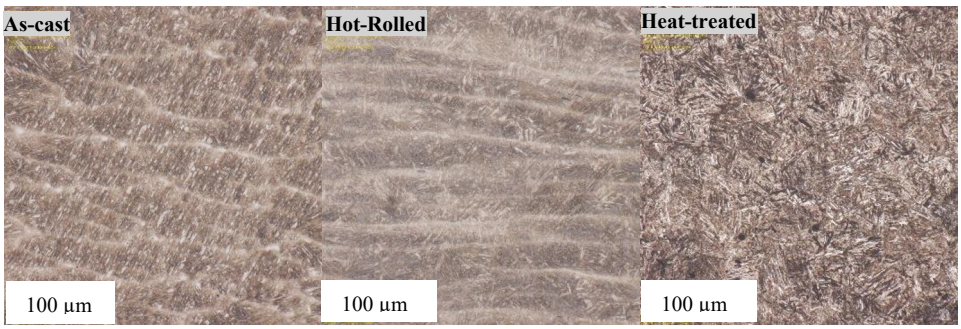

Fig. 2. The reference alloy in as-cast (left), hot-rolled (middle), and heat-treated (right) conditions, showing the effect of the rolling and heat treatment on the observed microstructure.

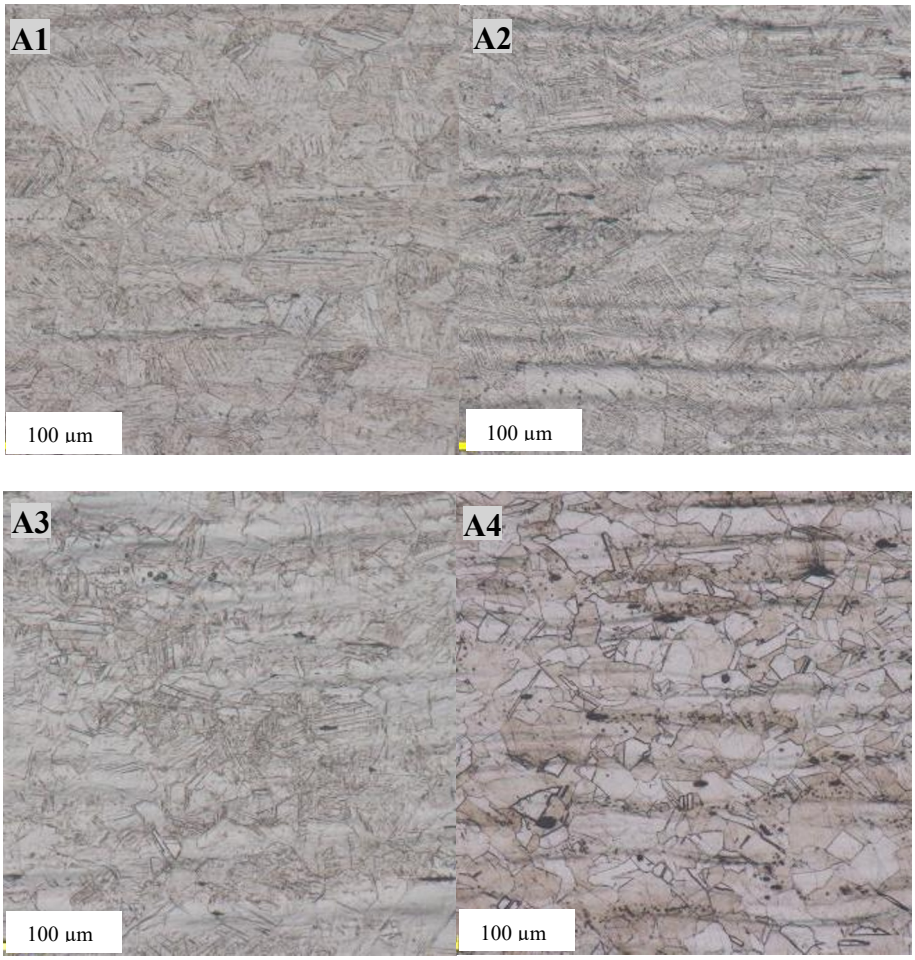

Fig. 3. Microstructure of hot rolled (HR) A1 (top left), A2 (top right), A3 (bottom left) and A4 (bottom right) alloys showing the austenitic matrix with some deformation twins.

3.2 Hardness and Charpy Impact

The hot rolled (HR) Alloys and Reference were tested at room temperature for hardness. A trend of a decrease in hardness with the increase in manganese was observed, Fig. 4. The impact of the same hot rolled alloys at room temperature showed an increase in impact energy with the increase in manganese. This supports the hardness results as the increase in hardness comes with a decrease in toughness. The increase in Mn content in Mn-based alloys is reported to enhance their strength and work hardening, improve ductility and toughness by increasing residual austenite (RA), and promote the formation of deformation twins during impact [7]. A balance between hardness and toughness is important for material performance. The tensile (UTS and yield) results will be used to benchmark the strength of the alloys.

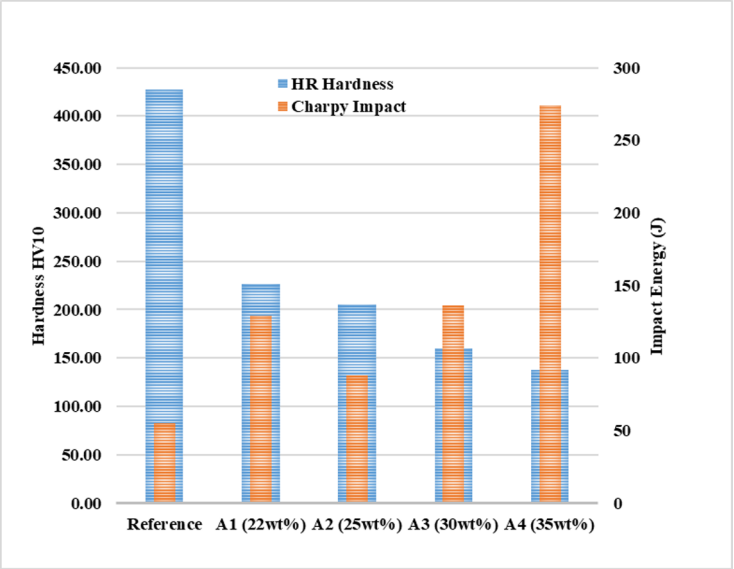

Fig. 4. Vickers hardness and the Charpy impact bar chart of HR reference and the FeMn binary alloys (A1 to A4) conducted at room temperature.

The hot rolled and heat-treated samples, including the Reference alloy, were tested at cryogenic temperatures (-196 °C). The comparison between the room and cryogenic temperature results of the hot rolled samples and heat-treated samples was done, and a drop in toughness was observed, Fig. 5. At room temperature, the toughness of all alloys was higher than at cryogenic temperatures and increased with the increase in Mn content. At -196 °C, the trend was consistent in both the hot-rolled (HR) and heat-treated (HT) condition samples; the toughness is lowest at 25 wt.% Mn-containing alloy. However, there is an observed toughness improvement upon increasing the Mn content above 25 wt.%. This trend is consistent with the hardness reported in the prior paper [8]. In understanding the reason for the drop in toughness at 25 wt.% Mn, SEM fractography needs to be conducted to assess the mode of failure, as it has been reported to contribute to the drop [5].

The heat-treated samples at cryogenic temperature showed a significantly lower impact toughness. This trend is true for A1, A2 and A3, but A4 showed a slight increase of 13.8% in toughness. This calls for an interrogation of the microstructure and fracture surfaces of the samples to understand this change. SEM and XRD will be used for microstructural and phase analysis. The specified Charpy impact energy for the Reference alloy in literature is 41J and 27J in HR-condition at -196°C in the transverse and longitudinal direction, respectively [9]. The observed value for the Reference alloy was 35J, which is slightly lower. All the binary Fe-Mn alloys were higher than the minimum of 41J in impact toughness in the hot rolled condition, except for A2 (25 wt.%) alloy. The impact toughness of A1, A3 and A4 alloys in HR condition at cryogenic temperatures was 45J, 48J, and 65J, respectively.

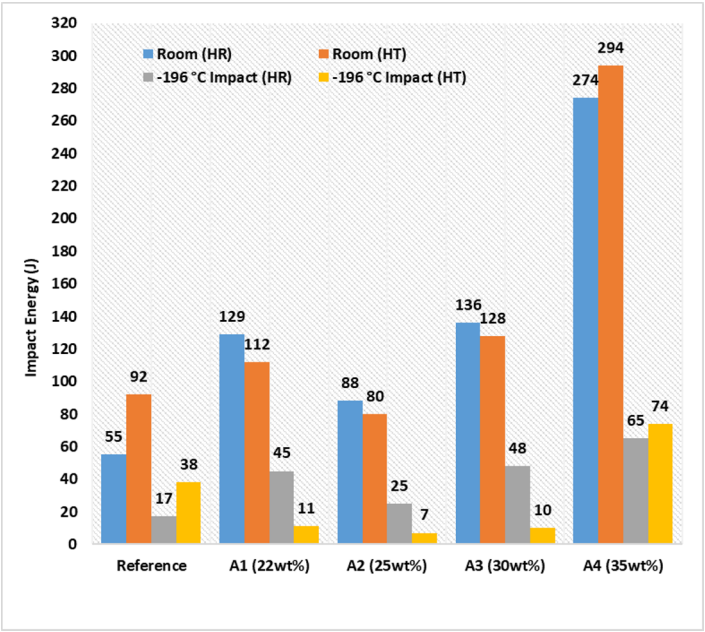

Fig. 5. Charpy impact of HR and HT reference and Fe-Mn binary alloys (A1 to A4) measured at room and cryogenic temperatures.

4 Conclusion

This work provides a platform to assess and compare the impact toughness obtained in binary FeMn-based alloys with varied Mn content and compare to 9 wt.% Ni. It was evident that alloys with the highest Mn content yielded the highest impact toughness, meeting the required minimum values at both room temperature (25 °C) and cryogenic temperature (-196 °C) testing conditions. From the studied alloy compositions, only the A4 sample with 35 wt.% Mn showed the best impact toughness of above 50 J against the minimum required value of 41J at cryogenic temperature testing upon both the HR and HT processes, whereas A1 and A3 complied only after HR condition.

The authors would like to acknowledge Mintek for funding, time and the platform to perform the research work and support. Wits for study opportunity and supervisory advice.

Data availability: Data can be made available upon request.

References

1. J. Xiong, E. Liu, C. Zhang, L. Kong, H. Yang, X. Zhang, Y. Wanget, Tuning mechanical behaviour and deformation mechanisms in high-manganese steels via carbon content modification, Mat. Sci. and Eng. A. **881,** 145401, (2023). https://doi.org/10.1016/j.msea.2023.145401
2. A. Asghari, A. Zarei-Hanzaki, and M. Eskandari, Temperature dependence of plastic deformation mechanisms in a modified transformation-twinning induced plasticity steel, Mat. Sci. and Eng. A, **579**, pp. 150–156, (2013). https://doi.org/10.1016/j.msea.2013.04.106

3. O.M. Akinbami, S.R. Oke, and M.O. Bodunrin, The state of renewable energy development in South Africa: An overview, Alex. Eng. J., **60** (6), pp. 5077–5093, (2021) https://doi.org/10.1016/j.aej.2021.03.065
4. K. Hickmann, A. Kern, U. Schriever and J. Stumpfe, Production and Properties of High Strength Nickel Alloy Steel Plates for Low Temperature Applications, (ThyssenKrupp Stahl AG, Division Metallurgy/Heavy Plate, Profit Centre Heavy Plate, Germany, 2005)
5. Y. Tomota, M. Strum, J. Morris Jr., Microstructural Dependence of Fe-High Mn Tensile Behaviour, Met. Trans. A. **18A**, (1986), 1073 https://doi.org/:10.1007/BF02643961
6. S-J. Oh, D. Park, K. Kim, I-J. Shon, S-J. Lee, Austenite stability and mechanical properties of nanocrystalline Fe–Mn alloy fabricated by spark plasma sintering with variable Mn content, Mat. Sci. and Eng. A. **725**, (2018) https://doi.org/10.24425/123833
7. Z. Zhan, Z. Shi, Z. Wang, W. Lu, Z. Chen, D. Zhang, F. Chai, X. Luo, Effect of manganese on the strength–toughness relationship of low-carbon copper and nickel-containing hull steel, Mat. **17**, 1012 (2024) https://doi.org/10.3390/ma17051012
8. L. Mampuru, M. Phasha, M. Bodunrin, D. Klenam, J. Moema, Microstructural characterisation and hardness of Fe-Mn alloys compared to commercial 9%Nickel alloy, MATEC Web Conf., **406**, 03018, (2024) https://doi.org/10.1051/matecconf/202440603018
9. International Association of Classification Societies, IRS, Guidelines on Approval of High Manganese Austenitic Steel for Cryogenic Service, (Indian Register of Shipping, India, September 2022).